MedChemComm

Accepted Manuscript

This article can be cited before page numbers have been issued, to do this please use: R. I. Storer, R. Owen, A. Pike, C. Benn, E. Armstrong, D. C. Blakemore, M. Bictash, K. Costelloe, E. Impey, P. Milliken, E. Mortimer-Cassen, H. Pearce, B. Pibworth and G. Toschi, *Med. Chem. Commun.*, 2016, DOI: 10.1039/C6MD00190D.

ROYAL SOCIETY OF CHEMISTRY

www.rsc.org/medchemcomm

View Article Online
DOI: 10.1039/C6MD00190D

Journal Name

ARTICLE

The discovery and evaluation of diaryl ether heterocyclic sulfonamides as URAT1 inhibitors for the treatment of gout†

Received 00th January 20xx,
Accepted 00th January 20xx

DOI: 10.1039/x0xx00000x

www.rsc.org/

R. Ian Storer,[a]* Robert M. Owen,[a] Andy Pike,[b]* Caroline L. Benn,[c] Emma Armstrong,[c] David C. Blakemore,[a] Magda Bictash,[c] Kathryn Costelloe,[c] Emma Impey,[c] Philip H. Milliken,[d] Elisabeth Mortimer-Cassen,[d,‡] Hannah J. Pearce,[e] Benjamin Pibworth,[f] Gianna Toschi[f]

Elevated serum uric acid levels can lead to gout which remains an area of unmet medical need. Following an unexpected clinical uricosuric effect observed with a sulfonamide compound, PF-05089771 (**9**), subsequently attributed to weak URAT1 inhibition, the optimization of a series of acidic sulfonamides as selective URAT1 inhibitors was undertaken. Compounds **10f** and **10i** were identified as suitable leads for more extensive profiling after exhibiting high URAT1 inhibitory potency and subsequently demonstrated promising preclinical ADME and safety profiles.

Introduction

Uric acid (**1**) is an endogenous metabolite resulting from the metabolism of purines and is also present in the diet. In most mammals, uric acid is principally cleared via metabolism to allantoin by the enzyme uricase. However, humans do not express functional uricase and the major route of uric acid clearance is via renal excretion. Hyperuricemia describes elevations in serum levels of uric acid (>6.0 mg/dL) which, despite often being asymptomatic, can lead to an increased risk of urate crystal formation due to the limited solubility of uric acid at these concentrations. At higher concentrations (>6.8 mg/dL), crystals of uric acid have the propensity to collect around the peripheral joints of the limbs leading to gout, a disease characterized by painful inflammatory joint flares. If untreated, crystal deposits called tophi can form and lead to irreversible damage to the joints.[1-6]

Hyperuricemia is commonly treated using xanthine oxidase (XO) inhibitors, allopurinol (**2**) and febuxostat (**3**), which reduce the rate of uric acid synthesis (Figure 1). However, an appreciable proportion of patients do not respond effectively to XO inhibitors.[1]

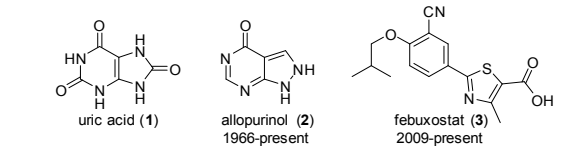

Figure 1. Uric acid (**1**) and XO inhibitor drugs.

An alternative approach to the reduction of serum uric acid levels is to increase renal clearance using uricosuric agents. Typically ≥90% of filtered urate is actively reabsorbed in the renal proximal tubule via organic anion transporters, principally URAT1 (*SLC22A12*).[7-8] Therefore, inhibition of URAT1 results in reduction of serum uric acid levels by increasing renal clearance. This has been demonstrated genetically, with non-functional missense mutations leading to hypouricemia, and pharmacologically by URAT1 inhibitors such as benzbromarone (**4**) and probenecid (**5**) (Figure 2).[9]

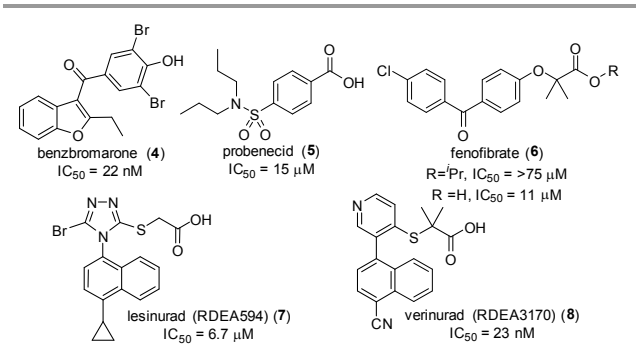

Figure 2. Clinical URAT1 inhibitors.

Benzbromarone (**4**) was first marketed for gout treatment in 1976, but withdrawn in 2003 due to compound-related

[a] Worldwide Medicinal Chemistry, [b] Pharmacokinetics Dynamics and Metabolism, [c] Discovery Biology, [d] Drug Safety, [e] Pharmaceutical Sciences, Research & Development, Pfizer Ltd, The Portway, Granta Park, Cambridge, CB21 6GS, UK.
[f] Peakdale Molecular Ltd, Discovery Park House, Ramsgate Road, Sandwich, Kent, CT13 9ND, UK.
* To whom correspondence should be addressed: RIS: *email: ian.storer@pfizer.com; AP:email: andy.pike@pfizer.com*
† The authors declare no competing interests.
‡ Current address: Global Head of Reguatory Safety, AstraZeneca, Melbourn Science Park, Hertfordshire, SG8 6EE, UK..
Electronic Supplementary Information (ESI) available: URAT1 assay protocol, experimental procedures, HPLC, MS, ^{1}H NMR, and ^{13}C NMR spectra of key compounds. See DOI: 10.1039/x0xx00000x

View Article Online
DOI: 10.1039/C6MD00190D

hepatotoxicity (Figure 2).[10-11] However, prior to withdrawal, benzbromarone (**4**) had been shown to be an effective treatment and proven successful in XO non-responding patients. Recently there has been renewed interest in uricosuric agents with a number of companies pursuing URAT1 inhibitors either by repurposing secondary uricosuric drugs such as fenofibrate (**6**) or by developing novel clinical agents.[12] Notable examples include lesinurad (RDEA594, **7**) and verinurad (RDEA3170, **8**), developed by Ardea Biosciences and later acquired by AstraZeneca with lesinurad gaining approval for treating gout in late 2015.[1]

Whilst developing a $Na_V1.7$ sodium channel inhibitor, PF-05089771 (**9**) (Figure 3), unexpected secondary effects on uric acid were observed in clinical trials: A decrease in serum urate was accompanied by an increase in urinary excretion. At doses of >450 mg b.i.d., where PF-05089771 (**9**) plasma C_{ave} unbound was ~60 nM, serum urate reduction approached ~50%, similar to that achieved by benzbromarone.[13] This effect was subsequently attributed to inhibition of URAT1 (IC_{50} = 3.5 μM).

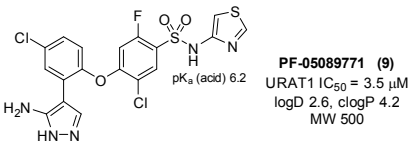

Figure 3. Clinical compound: secondary uricosuric effect.

Despite this interesting clinical result, a specific gout clinical trial was not undertaken with PF-05089771 (**9**). This was largely due to the high doses of the compound (>450 mg bid) required to deliver robust levels of efficacy, in combination with a complex 10-step synthesis, leading to a prohibitively high projected cost of goods for the gout marketplace. We therefore undertook the simplification and optimization of this acidic sulfonamide template towards improved URAT1 potency and herein describe a novel chemotype for URAT1 inhibition. However, the availability of the clinical data for PF-05089771 (**9**) proved useful in defining the desired target profile.

Determining the requisite potency level for advancing a compound was hampered by the lack of a valid preclinical model, due to the effect of uricase in non-human mammals. This dictated the use of existing clinical data as the only guide to the required potency. However, direct clinical PK/PD comparison between known uricosuric compounds is challenging, due to both the lack of consistent data sets and complicating factors such as active metabolites e.g. benzbromarone,[14] active renal excretion which may imply that ultrafiltrate concentrations in the proximal tubule significantly differ from unbound plasma e.g. lesinurad,[15-16] or potential organic anion transporter polypharmacology e.g. probenecid.[9, 17] However, for our clinical compound, PF-05089771 (**9**), and simple literature examples e.g. fenofibrate (**6**) (albeit this compound is a prodrug of fenofibric acid with the parent ester being essentially inactive in our hands) we tentatively rationalized the low fraction of IC_{50} required to drive efficacy using an E_{max}+baseline type response with the following assumptions:

1) The relevant effect is urate renal clearance, E_{max} and baseline are GFR and 5% of GFR respectively (normal urate renal clearance, although it should be noted that this number may not hold for individuals with highly elevated urate).
2) Unbound plasma concentration is a valid surrogate of the ultrafiltrate drug concentration in the proximal tubule.
3) Renal clearance is the only significant route of urate clearance in humans.

Results and Discussion

Although acidic sulfonamides are interesting acid isosteres due to potential to span a range of pK_a values they have not previously been described as URAT1 inhibitors. In order to capitalize on this finding, and in the absence of detailed structural biology information on the target binding site, a screening campaign of the company file was undertaken focusing on lower molecular weight (MW <450) and logD (<3) acids. In particular, an extensive compound legacy of diaryl ether sulfonamides existed from the $Na_V1.7$ program, which had originally delivered compound **9**. A bespoke set of 20k acidic compounds, rich in sulfonamides, was tested in a functional radiolabel proximity assay measuring uric acid uptake into URAT1 transfected cells (see supporting information). Pleasingly, this campaign delivered a high hit rate with 6% of compounds showing >30% inhibition at 10 μM.

Within these hits, a number of reasonably potent and lipophilic efficient acidic diaryl ether sulfonamides were identified as shown graphically in Figure 4.[18-19]

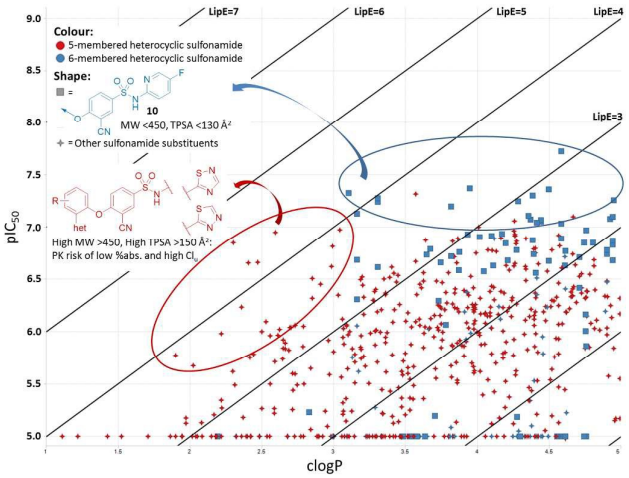

Figure 4. Screening campaign of diaryl ethers from company compound collection.

Interestingly, despite a diverse range of compounds being tested, derived from a range of different amino-heterocycles, sulfonamide core ring substitutions and diaryl ether substituents, the most lipophilic efficient hits fell broadly into two structural subseries. As highlighted in Figure 4, the first subseries was derived from 1,2,4- or 1,3,4-aminothiadiazoles, with a nitrile substituted core ring and diarylether motif comprising an ortho-heterocycle substitution.[18] This sub-series

View Article Online
DOI: 10.1039/C6MD00190D

of compounds generally exhibited high molecular weight (MW >450) and high TPSA (>150 Å^2) which resulted in low passive permeability (RRCK <5x10^{-6} cm/sec). Previous experience with compounds possessing similar physicochemical properties on the $Na_V1.7$ project suggested that this subseries would likely suffer from poor and unpredictable preclinical PK due to low absorption and high unbound clearance driven by organic anion-transporting polypeptide (OATP) mediated hepatic uptake.[20] As a result, this sub-series was not actively pursued.

The other efficient subseries from the initial compound screen was based on a 2-amino-5-fluoropyridine sulfonamide headgroup with a nitrile-substituted phenyl core (**10**).[19] These compounds were characterised by lower molecular weight (MW <450) and lower TPSA (<130 Å^2) which resulted in higher levels of passive permeability (RRCK >10x10^{-6} cm/sec). In addition, several of these hits already possessed good URAT1 potency (URAT1 IC_{50} = <100 nM) and promising levels of ligand efficiency (LE >0.35) and ligand lipophilic efficiency (lipE = ~4). As a result, this subseries became the main focus of further optimisation and characterisation work.

Table 1. Selected hits from initial screening campaign.

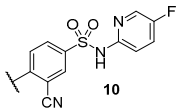

10

No.	Structure	URAT1 IC_{50} (nM)	LE (LipE)[a]	logD[b]	clogP	HLM[c] Cl_{int}
10a	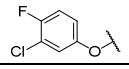	19 (n=7)	0.37 (3.2)	2.3	4.5	163
10b	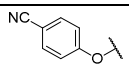	74 (n=5)	0.36 (3.9)	-	3.2	<8
10c	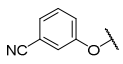	206 (n=2)	0.33 (3.5)	-	3.2	65
10d	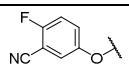	57 (n=12)	0.35 (3.9)	1.5	3.3	83
10e	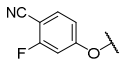	53 (n=12)	0.35 (4.0)	1.4	3.3	<8

[a]LipE = -log(IC_{50})-clogP; [b]logD shake flask octanol/H_2O; [c]HLM (μL/min/mg)

Example pyridine sulfonamides hits (**10**) are illustrated by selected compounds **10a-e** (Table 1). These all exhibited moderate to good lipophilic efficiencies (lipE = 3.2-4.0) and demonstrated promising potency in the IC_{50} = <100 nM range. However, the SAR for stability to oxidation in human liver microsomes proved interesting. As expected, more lipophilic and π-electron rich diaryl ether systems generally exhibited high rates of oxidation eg **10a** (HLM 163 μL/min/mg). Conversely, more polar and electron poor systems were generally more stable. However, a *p*-CN substituent appeared optimal for microsomal stability (comparing iso-lipophilic *p*-CN **10b** vs *m*-CN **10c**: HLM <8 vs 65 μL/min/mg respectively). Interestingly, this trend for superior HLM stability for *p*-CN vs *m*-CN also held for the corresponding fluorinated derivatives **10d** vs **10e** (HLM 83 vs <8 μL/min/mg).

Table 2. Selected compound optimisation.

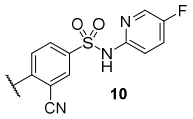

10

No.	Structure	URAT1 IC_{50} (nM)	LE (LipE)[a]	logD[b]	clogP	HLM[c] Cl_{int}
10f	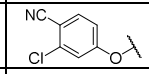	12 (n=27)	0.38 (4.2)	1.8	3.7	<13
10g	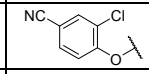	183 (n=8)	0.33 (3.1)	1.9	3.6	<8
10h	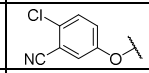	92 (n=2)	0.34 (3.3)	2.0	3.7	134
10i	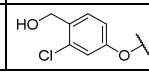	1 (n=9)	0.43 (5.6)	2.0	3.4	<10

[a]LipE = -log(IC_{50})-clogP; [b]logD shake flask octanol/H_2O; [c]HLM (μL/min/mg)

It was decided to optimise compounds from this subseries, maintaining the p-CN group for potency and oxidative metabolism stability characteristics. As fluorinated compound **10e** had shown moderate potency (URAT1 IC_{50} = 57 nM) and good HLM stability (<8 μL/min/mg), it was anticipated that the analogous Cl analogue **10f** should be approximately half a log unit more lipophilic and thereby ~5x more potent if lipE were maintained whilst retaining good stability to microsomal oxidation. As a result, compound **10f** was synthesised along with isomers **10g** & **10h** (Table 2). Pleasingly, compound **10f** exhibited lead-like levels of both URAT1 inhibition potency (IC_{50} = 12 nM) and microsomal stability (HLM <13 μL/min/mg). The direct isomers **10g** & **10h** were less promising, both exhibiting lower URAT1 inhibition potency. Also, as previously observed, compound **10h** with *m*-CN showed high microsomal turnover (HLM 134 μL/min/mg).

The diaryl ether ring system of **10** was further investigated for additional potential lipophilic efficiency gains. Surveying the broader SAR from the original screening campaign, an unoptimised example was noted where a para-hydroxymethyl substituent appeared to provide an improvement in lipophilic efficiency. As a result, this group was introduced into the preferred template to provide compound **10i**. Pleasingly, this hydroxymethyl group provided a significant improvement for compound **10i** in terms of both potency (URAT1 IC_{50} = 1 nM) and lipophilic efficiency (lipE = 5.6) as compared to compound **10f** (URAT1 IC_{50} = 12 nM, lipE = 4.2). Compound **10i** also maintained good microsomal stability (HLM <10 μL/min/mg), making this a suitable lead alongside compound **10f**.

Once initial lead compound (**10f**) had been identified, a systematic optimisation of the template was carried out (Table 3, compounds **11-26**). This included exploration of alternative 5- and 6-membered heterocycle sulfonamide headgroups and core ring substitutions.[18-19] However, although a number of derivatives were synthesised and tested, no improvements to either potency or lipophilic efficiency were observed suggesting the original core template (**10**) obtained from the original file mining and screening to be optimal.

View Article Online
DOI: 10.1039/C6MD00190D

Table 3. Selected sulfonamide heterocycle and core substitution SAR.

No.	Structure	URAT1 IC_{50} (nM)	LE (LipE)[a]	clogP
11	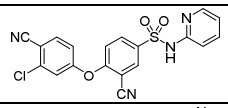	115 (n=4)	0.35 (3.3)	3.6
12	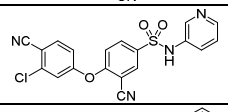	395 (n=3)	0.32 (2.8)	3.6
13	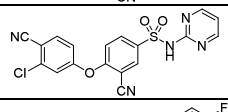	1823 (n=3)	0.29 (3.0)	2.7
14	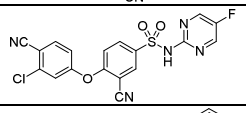	1954 (n=2)	0.28 (2.9)	2.8
15	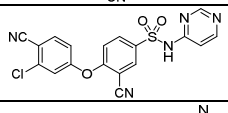	5147 (n=3)	0.26 (2.6)	2.7
16	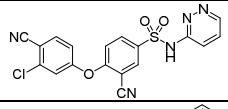	3868 (n=1)	0.27 (3.0)	2.4
17	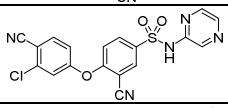	2982 (n=2)	0.28 (2.8)	2.7
18	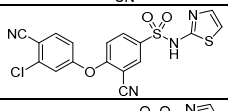	58 (n=3)	0.38 (3.8)	3.4
19	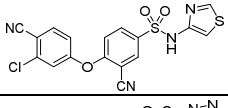	110 (n=2)	0.36 (3.6)	3.4
20	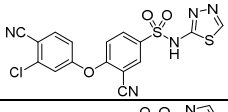	426 (n=5)	0.33 (4.0)	2.4
21	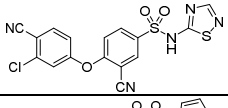	1123 (n=4)	0.31 (3.2)	2.7
22	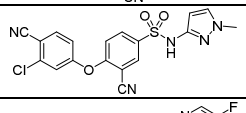	3358 (n=2)	0.27 (2.4)	3.1
23	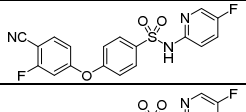	88 (n=1)	0.37 (3.5)	3.6
24	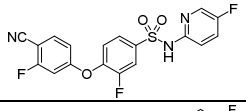	382 (n=3)	0.32 (2.8)	3.6
25	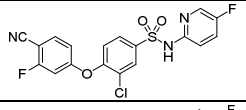	244 (n=1)	0.33 (2.4)	4.2
26	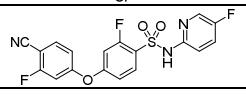	37 (n=3)	0.37 (3.6)	3.8

[a]LipE = -log(IC_{50})-clogP

Accordingly, compounds **10f** and **10i** were selected for further profiling. Both compounds were taken through in vitro ADME, safety and polypharmacology studies (Table 4).

Table 4. Broader profiles of lead compounds **10f** & **10i**

Property	Compound 10f	Compound 10i
Physicochemical properties		
Molecular weight (Da)	429	434
clogP / logD	3.7 / 1.8	3.4 / 2.1
pK_a	5.8	5.7
TPSA (Å)	124	121
Solubility at pH6.5 (μM)	7.7	15.3
ADME in vitro profiles		
RRCK ($x10^{-6}$ cm/sec)	16	12
P-gp efflux ratio	3.5	1.9
BCRP efflux ratio	122	34
HLM, Cl_{int} (μL/min/mg)	<13	<10
RLM, Cl_{int} (μL/min/mg)	<14	<14
DLM, Cl_{int} (μL/min/mg)	<18	<18
HHEP, Cl_{int} (μL/min/10^6 cells)	23	23
RHEP, Cl_{int} (μL/min/10^6 cells)	10	82
DHEP, Cl_{int} (μL/min/10^6 cells)	<6	<6
human plasma f_u	1.2×10^{-3}	8.3×10^{-3}
rat plasma f_u	2.1×10^{-3}	4.3×10^{-3}
dog plasma f_u	4.1×10^{-3}	1.4×10^{-2}
OATP cell uptake		
OATP1B1 (transfected/WT)	1.003	1.181
OATP1B3 (transfected/WT)	1.067	1.124
OATP2B1 (transfected/WT)	1.232	1.480
DDI CYP inhibition		
CYP1A2, inh. IC_{50} (μM)	>30	>30
CYP2C8, inh. IC_{50} (μM)	11.9	9.9
CYP2C9, inh. IC_{50} (μM)	4.2	2.0
CYP2C19, inh. IC_{50} (μM)	17.2	17.5
CYP2D6, inh. IC_{50} (μM)	>30	>30
CYP3A4, inh. IC_{50} (μM)	17.5	>30
Anion transporter inhibition		
OAT1 IC_{50} (μM)	14.0	14.3
OAT3 IC_{50} (μM)	0.72	0.5
OAT4 IC_{50} (μM)	14.0	15
Safety		
THLE cytotoxicity (μM)	103	105
IVMN (+/- S4)	negative	negative
Ames (+/- S4)	negative	negative
Ion channel pharmacology[a]		
hERG ephys. IC_{50} (μM)	67	>100
$Na_V1.5$ ephys. IC_{50} (μM)	>30	>30
$Na_V1.7$ ephys. IC_{50} (μM)	>30	>30
$GABA_A$ K_i (μM)	4.8	>10

[a]Full Cerep polypharmacology profiles included in SI section.

Pleasingly, neither compound appeared to present any serious liabilities in these assays. In terms of in vitro ADME, the compounds showed good levels of passive permeability in the RRCK cell line and metabolic stability in both human

View Article Online
DOI: 10.1039/C6MD00190D

microsomes and hepatocytes.[21] Although some inhibition of CYP2C9 was observed (**10f**, CYP2C9 IC_{50} = 4.2 μM; **10i**, CYP2C9 IC_{50} = 2.0 μM) this was still relatively weak in comparison to the primary pharmacology, so deemed to present low DDI risk. Both compounds also looked promising for safety with low cytotoxicity potential in a THLE cell line and negative results in both Ames mutagenicity and in vitro micronucleus genetic toxicity studies. Off-target risks were assessed through in vitro polypharmacology panels. Interestingly, compound **10f** did show some weak μM-level off-target activity in a few instances whereas compound **10i** showed no off-target pharmacology in the test panel (see supporting information for full polypharmacology panel profiles across both compounds). Both compounds were progressed into low dose i.v. and oral (p.o.) in vivo PK in rat and dog (Table 5).

Table 5. Preclinical PK for compounds **10f** & **10i**

Property	PF-05089771 9	Compound 10f	Compound 10i
Rat PK			
Dose i.v./p.o. (mg/kg)	1.0/3.0	0.76/2.3	1.0/3.0
Cl_p (mL/min/kg)	6.0	0.48	
Cl_u (mL/min/kg)	447	229	See text &
$T_{1/2}$ (h)	4.4	7.1	supporting
V_{ss} (L/kg)	1.3	0.25	information*
F (%)	27	100	
Dog PK			
Dose i.v./p.o. (mg/kg)	0.1/3.0	0.5/1.0	0.5/1.0
Cl_p (mL/min/kg)	4.8	0.39	1.3
Cl_u (mL/min/kg)	641	95	93
$T_{1/2}$ (h)	1.4	6.7	3.9
V_{ss} (L/kg)	0.31	0.18	0.27
F (%)	35	100	50

*Rat i.v. data for compound **10i** were highly variable and not suitable for the calculation of PK parameters.

The preclinical pharmacokinetics of the parent series of the $Na_V1.7$ blockers (typically high MW >450 and lipophilicity), were typically characterized by moderate to high Cl_p in rodents, driven by OATP transporter-mediated liver uptake and biliary clearance[22] of parent compound, and uncharacteristically high V_{ss} for acidic molecules, which may also partly reflect liver uptake.[23] While PF-05089771 (**9**) showed exceptional preclinical PK within the series, typically in vitro to in vivo extrapolation was challenging.

In contrast, **10f** demonstrated excellent PK in both rats and dogs with low Cl_u, low V_{ss}, typical of an acidic molecule, and very high oral bioavailability (Table 5). In contrast to the parent series, the biliary excretion in bile duct cannulated rats was low, with <0.5% of the dose excreted in bile as unchanged parent. Renal clearance was <<GFR x f_u in rats and dogs (~0.0001 mL/min/kg in both species), indicating net re-absorption and a low contribution to total clearance. The major oxidative metabolite in human microsomes and hepatocytes was an oxidation of the chlorophenyl ring, which was seen in trace quantities in rat and not present in dog. Evidence for formation of a potentially reactive species following loss of the chlorobenzonitrile moiety in combination with addition of glutathione was observed in human hepatocytes with the presence of a glutathione conjugate and subsequent breakdown products. However, it was present only in trace amounts in dog and was not detectable in rats (see SI for metabolite scheme).

Compound **10i**, while having excellent i.v. PK in dogs with low Cl_u and V_{ss}, showed highly variable i.v. PK in the rat (which precluded the calculation of accurate PK parameters) and variable oral PK in both species. Again, a limited contribution of biliary clearance was noted in bile duct cannulated rats with ~10% of the dose of compound **10i** excreted in bile as unchanged parent. In human microsomes and hepatocytes, the major metabolite was an oxidation of the hydroxymethyl group to the carboxylic acid. In rat hepatocytes, significant glucuronidation, believed to be of the hydroxymethyl group, was also noted.

The ratio of uptake rates between cell lines expressing human OATP1, OATP3, or OATP4, and wild-type was close to 1 for both compounds, suggesting a low contribution of OATP driven active hepatic uptake to the clearance.

Both compounds showed significant efflux by BCRP in bi-directional transport experiments and, in the case of **10f** a modest additional effect of P-gp. While at relatively high preclinical doses the compounds showed good oral absorption, this may in part reflect saturation of the efflux transporters and the possibility of efflux affecting absorption at low clinical dose levels cannot be ruled out.

Compounds **10f** and **10i** were synthesized on sufficient scale to advance to preclinical in vivo toxicology studies. The synthesis of all compounds was initially carried out in 2-steps starting from commercially available sulfonyl chloride **27** (Scheme 1). Amide formation with 5-fluoropyridin-2-amine provided common intermediate **28** that was subsequently converted to the final compounds **10a-i** via S_NAr displacement with the corresponding phenols **29**. For compound **10f,** this method proved high yielding and was directly scaled to provide 113 g of material in 50% yield over 2-steps and in >99% purity after recrystallization from ethyl acetate. However, although compound **10i** was initially prepared in an analogous manner using the primary alcohol containing phenol **29i**, this displacement proved low yielding (29% yield).

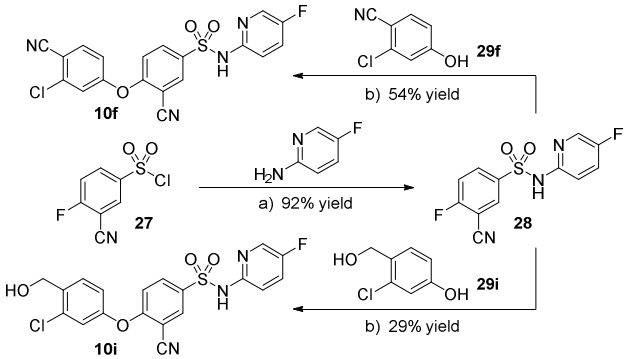

Scheme 1. (a) Pyridine, 23 °C, 2 h, (b) K_2CO_3, DMSO, 80 °C, recrystallization EtOAc.

View Article Online
DOI: 10.1039/C6MD00190D

In order to support larger scale synthesis, several alternatives were investigated for compound **10i**. It was anticipated that the main issue in the reaction was the unprotected benzyl alcohol. Disappointingly, protection of the benzyl alcohol with a silyl group, acetate group or dimethoxybenzyl group did not improve yields to any significant extent. However, adjustment of the oxidation level to the aldehyde or ester both proved effective in increasing the yield of the reaction. A screen of a range of bases identified K_3PO_4 and K_2HPO_4 to provide the cleanest reactions with K_2HPO_4 giving the highest overall yield. While K_2HPO_4 proved effective for the S_NAr with either the aldehyde or ester present, it was established that on scale-up, the cleanest and highest yielding reaction occurred in the presence of the aldehyde. As a result, aldehyde-containing phenol **29j** was applied to give S_NAr adduct **10j** in 77% yield. This was followed by subsequent reduction of the aldehyde to primary alcohol in 96% yield to provide the >250g of compound **10i** in a 68% yield over 3 steps.

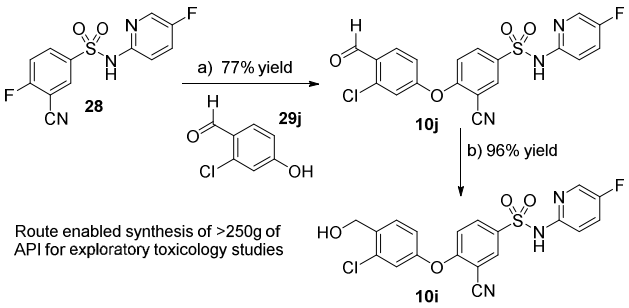

Scheme 2. (a) K_2HPO_4, DMSO, 100 ˚C, 2.5 h (b) $NaBH_4$, MeOH, rt, 45 min.

Both compounds **10f** and **10i** were taken into 14-day repeat-dose exploratory in vivo toxicity studies in rat and dog, with single-dose cardiovascular assessment in the rat. Compound **10f** was administered to both rats and dogs at 30, 100 and 300 mg/kg/day. In rat, compound related mortality was observed at 300 mg/kg/day and microscopic changes were noted in the kidney at 300 mg/kg/day (hypertrophy/hyperplasia of the urothelium and increased mitoses in the collecting ducts), and liver at ≥100 mg/kg/day (hepatocellular hypertrophy, with focal necrosis at 300 mg/kg/day). The maximum tolerated dose was therefore 100 mg/kg. On day 14 at the 30 mg/kg dose, at which there were no test article-related observations, unbound C_{max} and C_{ave} concentrations were 179 and 123 nM respectively. In dogs, compound **10f** was tolerated up to 300 mg/kg/day. Alanine aminotransferase (ALT) levels were decreased in males at doses ≥30 mg/kg/day and females at ≥100 mg/kg/day, without any pathologic correlation in the liver. A histologic change in testes was noted at 300 mg/kg/day, correlating with immaturity. However, evidence of testicular immaturity was also observed in the vehicle animal. On day 14 at the 30 mg/kg dose, unbound C_{max} and C_{ave} concentrations were 7419 and 3980 nM respectively. While some ALT observations were made at this dose, without pathological correlates, the exposure reached suggests an adequate therapeutic margin could be achieved. Cardiovascular assessment of compound **10f** in the rat at 10, 30 and 100 mg/kg identified a decrease in heart rate and body temperature at 10 mg/kg, with a small biphasic change in blood pressure (increase followed by decrease) at 30 and 100 mg/kg. The single dose unbound C_{max} and C_{ave} concentrations at the lowest dose of 10 mg/kg were 59 and 41 nM, respectively.

Similarly, compound **10i** was administered orally to rats at 30, 100 and 300 mg/kg/day and to dogs at 10, 30 and 100 mg/kg/day. In rats the compound was well tolerated up to 300 mg/kg/day and there were no test article-related clinical signs or changes in body weight, food consumption, hematology, clinical chemistry, organ weights, necropsy, or microscopic observations. At the 300 mg/kg dose unbound C_{max} and C_{ave} concentrations were 537 and 240 nM respectively. Similarly, in dogs compound **10i** was tolerated up to 100 mg/kg/day, and did not result in direct clinical pathology or histologic test article-related findings. Treatment related clinical signs of emesis and salivation were mainly present in high dose animals (100 mg/kg/day). Findings indirectly-related to treatment with **10i** were slightly decreased hepatic glycogen content and a decrease in serum glucose at 100 mg/kg, secondary to emesis. At the 100 mg/kg dose unbound C_{max} and C_{ave} concentrations were 3905 and 1019 nM respectively. Cardiovascular assessment of compound **10i** was conducted in the rat at 3, 30, and 100 mg/kg, with no adverse effects observed up to 30 mg/kg but an increase in blood pressure was observed at 100 mg/kg. The single dose unbound C_{max} and C_{ave} concentrations at the 30 mg/kg no cardiovascular effect dose were 98 and 43 nM, respectively.

Conclusions

In summary, the first example of a series of potent acidic sulfonamide URAT1 inhibitors is described. Following elucidation that clinically efficacious diaryl ether sulfonamide compound **9** likely derived its uricosuric activity via inhibition of URAT1, this template was subsequently optimized for lower molecular weight, lipophilicity and synthetic complexity. This led to the design of potent sulfonamide compounds **10f** and **10i**. Profiling through detailed in vitro and in vivo preclinical ADME and safety studies highlighted that both compounds **10f** and **10i** exhibited promising preclinical PK and safety profiles making them interesting candidates for possible further development with the principal issues being the potential formation of reactive species for **10f** and low confidence in human PK prediction for **10i**. In the event, further refinement of the series produced more favourable compounds which are the subject of a separate manuscript.[24]

Acknowledgements

We thank Joe Warmus for assistance with compound characterization, Peakdale Molecular Ltd for the synthesis of compound analogues and York Bioanalytical Solutions for the generation of ADME data. We also thank Laura Kammonen

View Article Online
DOI: 10.1039/C6MD00190D

and Paula Cawkill for cell culture and thank Katrina Gore and Phil Stanley for statistical data analysis support.

Abbreviations

ADME, absorption, distribution, metabolism and excretion; BCRP, breast cancer resistance protein; C_{ave}, average plasma concentration; C_{max}, maximum plasma concentration; Cl_p, plasma clearance; Cl_u, unbound clearance; CYP, cytochrome P450; DDI, drug-drug interaction; DHEP, dog hepatocytes; DLM, dog liver microsomes; F, bioavailability; f_u, fraction unbound; GFR, glomerular filtration rate; HHEP, human hepatocytes; HLM, human liver microsomes, IC_{50}, half-maximum inhibitory concentration; IVMN, in vitro micronucleus; LE, ligand efficiency; LipE, lipophilic efficiency; OAT, organic anion transporter; OATP, organic anion-transporting polypeptide; PD, pharmacodynamics; P-gp, P-glycoprotein; PK, pharmacokinetics; ppb, plasma protein binding; RHEP, rat hepatocytes; RLM, rat liver microsomes; RRCK, Ralph Russ canine kidney cell line; SLC, solute carrier; SNAr, nucleophilic aromatic substitution; sUA, serum uric acid; $T_{1/2}$, half life; TPSA, topological polar surface area; V_{ss}, apparent volume of distribution at steady state

Experimental Section

In vitro assays

Full assay protocol for the URAT1 assay is provided in the supporting information.

In vivo studies

All experiments involving animals were conducted in our AAALAC-accredited facilities and were reviewed and approved by the Pfizer Institutional Animal Care and Use Committee. The acute rat toleration study was conducted by TCG Life Sciences (TCGLS). TCGLS adheres to the ethical guidelines of Committee for the Purpose of Control and Supervision of Experiments on Animals (CPCSEA), Govt. of India under the supervision of a fully compliant Institutional Animal Ethics Committee (IAEC).

General chemistry experimental

Details of general methods, experimental details for compounds, HPLC conditions and spectra for lead compounds **10f** and **10i** can be found in the supporting information. Selected experimental details for the synthesis of compounds **10f** and **10i** only are outlined below.

4-(3-Chloro-4-cyanophenoxy)-3-cyano-*N*-(5-fluoro-pyridin-2-yl)benzenesulfonamide (10f)

A mixture of 3-cyano-4-fluoro-*N*-(5-fluoropyridin-2-yl)benzenesulfonamide (**28**, 110 g, 0.38 mol), 2-chloro-4-hydroxybenzonitrile (**29f**, 85.8 g, 0.56 mol) and K_2CO_3 (154 g, 1.12 mol) in DMSO (1.1 L) was heated to 80 °C for 32 h, then stirred for an additional 16 h at rt. The reaction mixture was poured in to water (3 L). The combined organic layers were washed with water (1 L), citric acid solution (117 g, in 3.5 L, 3% w/w, 1.5 mol of citric acid for 1 mol of product) and water (1 L). The organic phase was concentrated in vacuo to give crude material (136 g). The compound was crystallised from EtOAc (1.6 L, 12 mL/g) to give material (110 g). This material was combined with 35 g of previously obtained material then partially dissolved in boiling ethyl acetate (~1.5 mL, 10 mL/g ca.). The mixture was left to cool overnight to room temperature and filtered to afford the title compound as a white solid (**10f**, 113 g, 54%). ^{1}H NMR (400 MHz, d6-DMSO) δ 11.34 (br. s., 1H), 8.44 (d, *J*= 2.34 Hz, 1H), 8.22 (d, *J*= 2.73 Hz, 1H), 8.16 (dd, *J*= 2.30, 9.00 Hz, 1H), 8.13 (d, *J*= 8.59 Hz, 1H), 7.83 (d, *J*= 2.34 Hz, 1H), 7.71 (ddd, *J*= 3.10, 8.60, 8.60 Hz, 1H), 7.47 (dd, *J*= 2.34, 8.98 Hz, 1H), 7.32 (d, *J*= 8.98 Hz, 1H), 7.13 (dd, *J*= 3.90, 8.98 Hz, 1H); ^{13}C NMR (101 MHz, d6-DMSO) δ 160.6, 158.6, 155.2 (d, *J*= 248.0 Hz), 148.0, 138.0, 137.2, 137.0, 135.6 (m), 134.6, 134.0, 126.8 (d, *J*= 22.7 Hz), 122.4, 120.4, 119.1, 116.1, 114.8, 114.6 (d, *J*= 4.40 Hz), 109.7, 104.2; ^{19}F NMR (376 MHz, d6-DMSO) δ -134.44: HPLC (system 1, 4.5 min, acid) R_t 3.03 min, ELSD >95% purity; LRMS m/z 428.95 $[MH]^+$; HRMS (ESI) *m/z*: $[MH]^+$ Calcd for $C_{19}H_{10}ClFN_4O_3S$ 429.0219, found 429.0221.

4-(3-Chloro-4-(hydroxymethyl)phenoxy)-3-cyano-*N*-(5-fluoropyridin-2-yl)benzene sulfonamide (10i)

To a suspension of 4-(3-chloro-4-formylphenoxy)-3-cyano-*N*-(5-fluoropyridin-2-yl) benzenesulfonamide (**10j**, 276.9 g, 0.64 mol) in methanol (5.5 L) at 0 °C was added $NaBH_4$ portion-wise over 25 min. The reaction was stirred at rt for 1.5 h, cooled to 0 °C then water (4.8 L) slowly added. The reaction mixture was warmed to rt and 1M HCl (2.5 L) was slowly added resulting in a suspension of the product. The mixture was left to stir at rt for 1 h and then the suspension was filtered and dried for 16 h at 40 °C under vacuum to give crude product. The crude product was dissolved in acetone (2.5 L) and then silica (380 g) was added to the vessel. The mixture was stirred at rt for 20 min and then filtered through a silica pad and washed with acetone (1.5 L). Water (10 L) was slowly added resulting in the precipitation of the product. The mixture was left to stir at rt for 1 h and then the suspension was filtered and the residue dried overnight at 40 °C to yield 4-(3-chloro-4-(hydroxymethyl)phenoxy)-3-cyano-*N*-(5-fluoropyridin-2-yl)benzenesulfonamide as a cream powder (**10i**, 268.2 g, 96%). ^{1}H NMR (400 MHz, d6-DMSO) δ 11.31 (br. s., 1H), 8.39 (d, J= 2.34 Hz, 1H), 8.22 (d, *J*= 2.73 Hz, 1H), 8.12 (dd, *J*= 2.34, 8.98 Hz, 1H), 7.70 (dd, *J*= 8.60, 3.10 Hz, 1H), 7.66 (d, *J*= 8.59 Hz, 1H), 7.48 (d, *J*= 2.73 Hz, 1H), 7.30 (dd, *J*= 2.34, 8.59 Hz, 1H), 7.12 (dd, *J*= 3.51, 8.98 Hz, 1H), 7.05 (d, *J*= 8.90 Hz, 1H), 5.50 (t, *J*= 5.46 Hz, 1H), 4.59 (d, *J*= 5.07 Hz, 2H); ^{13}C NMR (101 MHz, d6-DMSO) δ 162.48, 156.42 (d, *J*= 247 Hz), 152.96, 147.99, 138.19, 135.63 (d), 135.54, 134.66, 133.88, 132.52, 130.17, 126.88 (d, *J*= 19.1 Hz), 121.82, 120.02, 117.05, 115.11, 114.54 (d, *J*= 5.14Hz), 102.89, 60.38; 19F NMR (376 MHz, CDCl3) δ -134.5: HPLC (system 1, 25 min, acid) R_t 14.09 min, ELSD 98.9% purity; LRMS *m/z* 434.02 $[MH]^+$; HRMS (ESI) m/z: $[MH]^+$ Calcd for $C_{19}H_{13}ClFN_3O_4S$ 434.0372, found 434.0369.

View Article Online
DOI: 10.1039/C6MD00190D

4-(3-Chloro-4-formylphenoxy)-3-cyano-*N*-(5-fluoropyridin-2-yl)benzenesulfonamide (10j)

A suspension of 3-cyano-4-fluoro-*N*-(5-fluoropyridin-2-yl) benzene sulfonamide (**28**, 108.2 g, 0.37 mol), K_2HPO_4 (191.3 g, 1.10 mol) and 2-chloro-4-hydroxybenzaldehyde (**29j**, 63.1 g, 0.40 mmol) in DMSO (760 mL) was heated to 100 °C and left to stir for 2.5 h then cooled to rt. The reaction mixture was poured into water (3.0 L) resulting in some precipitation of product. EtOAc (3.0 L) was added and the aq. layer acidified to pH 3 using conc. HCl. The aq. layer was removed and the resulting suspension filtered and solid washed with EtOAc (200 mL) and 1M HCl (20 mL) to give crude product. The organic filtrates were retained and washed with 1M HCl (700 mL) and sat. brine (2 × 700 mL) and dried over $MgSO_4$, filtered and concentrated to yield more crude product. Both batches of crude product were combined and slurried in EtOAc (750 mL) at reflux for 45 min. The mixture was cooled to rt, filtered and the solid washed with EtOAc (2× 100 mL). The product was died overnight under vacuum at 40 °C to yield 4-(3-chloro-4-formylphenoxy)-3-cyano-N-(5-fluoropyridin-2-yl)benzene sulfonamide (**10j**, 121.1 g, 77%) as a cream powder. ^{1}H NMR (400 MHz, d6-DMSO) δ 11.34 (br. s, 1H), 10.28 (s, 1H), 8.42 (d, *J*= 2.3 Hz, 1H), 8.20 (d, *J*= 3.1 Hz, 1H), 8.14 (dd, *J*= 9.0 Hz, 2.4 Hz, 1H), 7.95 (d, *J*= 8.6 Hz, 1H), 7.69 (td, *J*= 8.6 Hz, 3 Hz, 1H), 7.63 (d, *J*= 2.4 Hz, 1H), 7.38 (dd, *J*= 8.2, 2.5 Hz, 1H), 7.28 (d, *J*= 8.9 Hz, 1H), 7.09 (dd, *J*= 9.2, 3.7 Hz, 1H); ^{19}F NMR (376 MHz, d6-DMSO) δ -134.4; HPLC (system 1, 4.5 min, acid) R_t 3.58 min, ELSD >95% purity; LRMS m/z 432.09 $[MH]^+$.

3-Cyano-4-fluoro-*N*-(5-fluoropyridin-2-yl)benzene sulfonamide (28)

3-Cyano-4-fluorobenzene-1-sulfonyl chloride (**27**, 60.3 g, 274 mmol) was added to a solution of 5-fluoropyridin-2-amine (40.0 g, 357 mmol) and pyridine (67 mL, 823 mmol) in DCM (1 L) at rt then stirred for 3 h. The solvent was removed under vacuum and the residue stirred in dilute HCl (2N, 850 mL) for 16 h. The precipitate was removed by filtration and the residue washed with water (200 mL) and dried under high vacuum overnight. The crude material was triturated with TBME (500 mL) to give the title compound (**28**, 70.3 g, 87%) as an orange solid. ^{1}H NMR (400 MHz, d6-DMSO) δ 11.45 (bs, 1H), 8.44 (dd, *J*= 6.0, 2.4 Hz, 1H), 8.26-8.24 (m, 1H), 8.18 (d, *J*= 3.2 Hz, 1H), 7.72-7.66 (m, 2H), 7.11-7.08 (m, 1H); ^{19}F-NMR (376 MHz, d6-DMSO) δ -101.50, -134.20: HPLC (system 2, 4.5 min, acid) R_t 2.55 min, ELSD >95% purity; LRMS m/z 296.06 $[MH]^+$.

References

1. C. Diaz-Torne; N. Perez-Herrero; F. Perez-Ruiz *Curr. Opin. Rheumatol.,* **2015,** *27*, 164.
2. H. Shahid; J. A. Singh *Expert Opin. Invest. Drugs,* **2015,** *24*, 1013.
3. M. H. Bach; P. A. Simkin *Curr. Opin. Rheumatol.,* **2014,** *26*, 169.
4. N. L. Edwards; A. So *Rheum. Dis. Clin. North. Am.,* **2014,** *40*, 375.
5. D. B. Crittenden; M. H. Pillinger *Annu. Rev. Med.,* **2013,** *64*, 325.
6. J. A. Singh *Expert Opin. Emerg. Drugs,* **2012,** *17*, 511.
7. Y. Lu; T. Nakanishi; I. Tamai *Drug Metab. Pharmacokinet.,* **2013,** *28*, 153.
8. T. Nakanishi; K. Ohya; S. Shimada; N. Anzai; I. Tamai *Nephrol., Dial., Transplant.,* **2013,** *28*, 603.
9. K. Maeda; Y. Tian; T. Fujita; Y. Ikeda; Y. Kumagai; T. Kondo; K. Tanabe; H. Nakayama; S. Horita; H. Kusuhara; Y. Sugiyama *Eur. J. Pharm. Sci.,* **2014,** *59*, 94.
10. A. Felser; P. W. Lindinger; D. Schnell; D. V. Kratschmar; A. Odermatt; S. Mies; P. Jeno; S. Krahenbuhl *Toxicology,* **2014,** *324*, 136.
11. M.-H. H. Lee; G. G. Graham; K. M. Williams; R. O. Day *Drug Saf.,* **2008,** *31*, 643.
12. D. Uetake; I. Ohno; K. Ichida; Y. Yamaguchi; H. Saikawa; H. Endou; T. Hosoya *Intern. Med.,* **2010,** *49*, 89.
13. Z. Ali; K. J. Butcher; R. P. Butt; S. J. Felstead; S. Glatt; R. M. McKernan; M. Panesar, **2013**, WO2013057722.
14. S. Uchida; K. Shimada; S. Misaka; H. Imai; Y. Katoh; N. Inui; K. Takeuchi; T. Ishizaki; S. Yamada; K. Ohashi; N. Namiki; H. Watanabe *Drug Metab. Pharmacokinet.,* **2010,** *25*, 605.
15. Z. Shen; C. Rowlings; B. Kerr; V. Hingorani; K. Manhard; B. Quart; L.-T. Yeh; C. Storgard *Drug. Des. Devel. Ther.,* **2015,** *9*, 3423.
16. http://www.accessdata.fda.gov/drugsatfda_docs/label/2015/207988lbl.pdf.
17. Y. Hagos; D. Stein; B. Ugele; G. Burckhardt; A. Bahn *J. Am. Soc. Nephrol.,* **2007,** *18*, 430.
18. R. M. Owen; R. I. Storer, **2014**, WO2014170793.
19. R. I. Storer; N. A. Swain; R. M. Owen, **2014**, WO2014170792.
20. H. M. Jones; R. P. Butt; R. W. Webster; I. Gurrell; P. Dzygiel; N. Flanagan; D. Fraier; T. Hay; L. E. Iavarone; J. Luckwell; H. Pearce; A. Phipps; J. Segelbacher; B. Speed; K. Beaumont *Clin. Pharmacokinet.,* **2016**, Ahead of Print.
21. L. Di; C. Whitney-Pickett; J. P. Umland; H. Zhang; X. Zhang; D. F. Gebhard; Y. Lai; J. J. Federico; R. E. Davidson; R. Smith; E. L. Reyner; C. Lee; B. Feng; C. Rotter; M. V. Varma; S. Kempshall; K. Fenner; A. F. El-kattan; T. E. Liston; M. D. Troutman *J. Pharm. Sci.,* **2011,** *100*, 4974.
22. K. M. Giacomini; S.-M. Huang; D. J. Tweedie; L. Z. Benet; K. L. R. Brouwer; X. Chu; A. Dahlin; R. Evers; V. Fischer; K. M. Hillgren; K. A. Hoffmaster; T. Ishikawa; D. Keppler; R. B. Kim; C. A. Lee; M. Niemi; J. W. Polli; Y. Sugiyama; P. W. Swaan; J. A. Ware; S. H. Wright; S. Wah Yee; M. J. Zamek-Gliszczynski; L. Zhang *Nat. Rev. Drug Disc.,* **2010,** *9*, 215.
23. A.-K. Sohlenius-Sternbeck; U. Fagerholm; J. Bylund *Xenobiotica,* **2013,** *43*, 671.
24. A. Pike; R. I. Storer; R. M. Owen; E. Armstrong; C. L. Benn; M. Bictash; K. Cheung; K. Costelloe; E. Dardennes; E. Impey; P. H. Milliken; E. Mortimer-Cassen; H. J. Pearce *MedChemComm,* **2016**, Submitted.

View Article Online
DOI: 10.1039/C6MD00190D

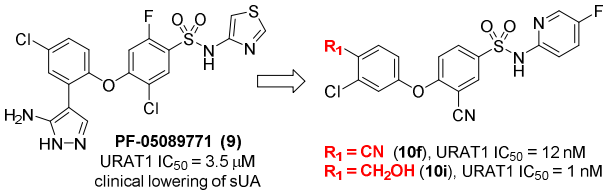

The discovery and optimization of a series of acidic heterocyclic sulfonamides that are potent and selective URAT1 inhibitors is described.